J. Pharm. Tech. Res. Management Vol. 10, No. 1 (2022), pp.47–73

CHITKARA

Journal of Pharmaceutical Technology Research and Management

Journal homepage: https://jptrm.chitkara.edu.in/

In Silico ADMET and Docking Study of Selected Drug Used in Therapy of COVID-19

Sagar Ashok Jadhav, Payal Pandurang Chavan, Supriya Suresh Shete, Dipti Shantisagar Patil, Saroj Dyandev Kolekar, Godfrey Rudolph Mathews, Dipak Babaso Bhingardeve and Pravin Kondiba Pawar

[1]*Dr. Shivajirao Kadam College of Pharmacy, Baganvat, Kasabe Digraj Sangli, Maharashtra - 416305, India*

[*]jsagar72@yahoo. (Corresponding Author)

ARTICLE INFORMATION

Received: August 10, 2021
Revised: October 15, 2021
Accepted: November 20, 2021
Published Online: May 07, 2022

Keywords:
Docking, AUTO-DOCK VINA, PYMOL

DOI: 10.15415/jptrm.2022.101006

ABSTRACT

Docking is one of the most widely utilized technique used method in structure -based drug design because of its capability to predict the binding conformation of ligands to appropriate target. Ability of binding/ affinity towards the target i.e., bioactive peptides or specific receptor provides strong evidence of binding conformation pattern and affinity for further investigation. Aim- The present study was conducted for evaluation of current API's potential used in COVID-19. Methods: In-silico molecular docking was performed using softwares such as SWISS ADME, MOLSOFT, MOLINSPIRATION, PYMOL, AUTO-DOCK VINA AND BIOVIA DS VISUALIZER. Results: The current research comprehend the drug likeliness character of selected API's and their binding affinity with various targets selected by SWISS TARGET PREDICTION. Conclusion: The present investigation suggests that all the targets follow Lipinski rule of five except Remdesivir and Anakinra besides which it possesses enhanced binding affinity toward targets, the binding energy of the protein ligand interaction additionally confirms that the ligand fits into the dynamite pockets which proves to be evident for further in- vivo and in-vitro evaluations..

1. Introduction

The severe acute respiratory syndrome coronavirus 2 (SARS-CoV2) outbreak was first noted in Wuhan, Hubei province, China (Pal M. et.al, 2020). This virus originated in Wuhan, China, and has since spread to more than 200 nations, with Brazil and the United States serving as the current epicenters. (Zheng J, 2020) According to data available as of June 18, 2020, at 4:57 p.m. CEST, COVID-19, which was caused by SARS-CoV2, has killed up to 4, 45, 535 people worldwide and affected 82, 42, 999 people (WHO coronavirus disease Dashboard). There are three types of coronaviruses, including SARS-CoV2, are responsible for lethal pneumonia in humans. The beta coronavirus family of Corona viridae contains the enclosed, positive sense single-strand RNA known as SARS-CoV2. Out of the three types, SARS-CoV2 is more contagious as compared to the other two, spreads the infection more rapidly and severely, resulting in large number of deaths which created a pandemic situation in 2020 (Malik Y A, 2020).

The SARS-COV2 genome is about 29 to 30 kb in length and is present in the corona virus structural protein, which is essential for its replication and transcription during infection. (V'kovski P, Kratzel, A et.al,2020). A main protease that cleaves nearly 790 kDa at more than 10 different sites. Mpro, a homodimer with two identical chains of Leu-Gln; Ser, Ala, and Gly are the recognition sequence. The Cys-His dyad protease, which cleaves Mpro, utilizes the cysteine's-SH group as a nucleophile throughout the cycle of proteolysis (Shrivastav V. et. al., 2022). Inhibiting the primary protease activity would prevent transcription or replication. By addition to the Cys145-His41 dyad, the active site of Mpro additionally comprises Phe140, Thr45,Arg188, Asp187, Met49, Asn142, Met165, Gln189, His172, and Glu166 residues of amino acids that are essential in substrate binding. (Antonopoulou lo. et. al., 2022). Molecular docking which an part bioinformatics-based research is consistently used to built framework and predict non-covalent interactions (mostly hydrogen bonding) between receptors (macromolecules) and ligand (drug molecule) (Morris GM. et. al., 2008). AUTO-DOCK is a programme for virtual screening and docking because it automatically calculates the grid for the required atom types. AUTO-DOCK VINA, an updated version, in orders of magnitude is more efficient than the original AUTO-DOCK4 and reaches binding pose prediction accurately within the average range.(Trotto et. al., 2010). When a structure is authentic, it provides drug-related data and, through various modifying features, draws attention to a number of characteristics that provide a large risk of adverse

ISSN No.: 2321-2217(Print) ISSN No.: 2321-2225(Online); Registration No. : CHAENG/2013/50088

consequences, such as poor absorption, genotoxicity, or drug conform behavior. (Homayun B. et. al., 2019). We can also determine the compounds' hydrophilicity, as well as the clog P (logarithm of compounds partition coefficient between water and n-Octanol) as per shown in table no 2. When the hydrophilicity is low and the clogP values are high, penetration and absorption are worse. Log S represents solubility; a lower log S value implies better solubility, which enhances absorption. The topological polar surface area (TPSA) of the compound indicates the surfaces of the polar molecules and atoms. Higher TPSA score implies lower membrane permeation and lower TPSA score are associated with enhanced penetration which to export of drug from cells as well as passes CNS. Another factor is toxicity, which frequently has a significant impact and regulates how drugs are absorbed, distributed, metabolized, and excreted. (Bojarska j. et. al., 2020). ADMET and drug-likeness predictions support in silico discovery of novel targets and compounds with expected biological activity. The main objective of this study is to perform molecular docking evaluation of the COVID-19 active API's. This evaluation will be guided by various molecular research (hydrogen bond prediction between target and drugs), druglikeness behaviour, and ADMET estimation in order to determine the effectiveness and efficacy of such active compounds against SARS-CoV2. (Vardhan S. et. al., 2020). The creation of strong, affordable computer tools has revolutionised science and medicine. Different drug designs are now often used in academic and professional settings. In silico drug-receptor candidate interaction screening, also known as virtual high-throughput screening (vHTS), has gained appeal as a tool for drug discovery. Compounds are rated and ranked according to their expected physicochemical properties and drug-receptor compatibility utilising information filters including molecular weight, the number of hydrogen bonds, hydrophobicity, and penalty functions. (Eknis S. et. al., 2007). A far more focused approach has lately been used to address these concerns in the early stages of design, even though medicinal chemists are aware of absorption, distribution, metabolism, elimination, and toxicity (ADMET or ADME/Tox). Many predictive ADME simulations employ quantitative structure activity relationships (QSAR)(Lin J. et. al., 2003). There is an increasing need to find new COVID-19 medications because serious illnesses like corona are emerging so quickly. To solve this problem, we developed a deep neural network that can predict compounds with antiviral activity using both the ADMET screening and the docking score. For this attention the current research is concentrated on COVID-19 (Sharma A. et. al., 2020)

2. Material and Method

2.1. Preparation of Ligands

The 2D structures (.mol) of all compounds were drawn by using CHEMDRAW software. All 2D structures were converted to 3D structure (pdb) by using PYMOL software. The 3D coordinates (.pdb) of each molecule were loaded on to Chem3D for energy minimization. (Herowati. R. et. al., 2012).

2.2. Preparation of Macromolecule

The protein targets retrieved from the RCSB protein data bank are (PDB code: 3O1G, 4B72, 4B78, 4YJU, 5LH4, 1JD0, 4QJ0, 4QJW, 6G5L, 6G7A, 3UEG, 3UGD, 3UGI, 5TTU, 6DUD, 2VCV, 3L9W, 5VLO, 5VN1, 6NSD, 4RFZ, 5JRS, 5KUP, 5OTQ, 5P9I) which serves as docking receptors. All the bound ligands and water molecules were removed from the active site of the receptor as well as hydrogen bonds were added by using BIOVIA DISCOVERY STUDIO.

2.3. Molecular Docking Analysis (AUTO DOCK VINA)

The molecular docking studies were carried out using AUTO-DOCK TOOLS (ADT) version: 4.2 (1.5.6), which is a free graphic user interface (GUI) for the AUTO-DOCK VINA program. AUTO-DOCK VINA with standard protocol was used to dock the marketed selected drugs against the active site of protein (PDBID: 3O1G, 4B72, 4B78, 4YJU, 5LH4, 1JD0, 4QJ0, 4QJW, 6G5L, 6G7A, 3UEG, 3UGD, 3UGI, 5TTU, 6DUD, 2VCV, 3L9W, 5VLO, 5VN1, 6NSD, 4RFZ, 5JRS, 5KUP, 5OTQ, 5P9I) as per shown in fig 1-24. Nine different conformations were generated for each ligand scored using AUTO-DOCK VINA scoring functions and ranked according to their binding energies. Segregation of best pose was done by using AUTO-DOCK SPLIT software. AUTO-DOCK TOOLS, BIOVIA DISCOVERY STUDIO and PYMOL were used for the post-docking analyses. The conformations with the most favorable (least) free binding energy were selected for analyzing the interactions between the target receptor and ligands by PYMOL. (Rauf. MA. et. al., 2015).

2.4. In silico Drug-Likeness Predictions

In accordance with the method described by Amina et. al., (2016), the structures of all chosen commercially available drugs were submitted to the SWISS ADME TOOL and converted to their canonical simplified molecular input line entry system (SMILE). This allowed for the estimation of

in silico pharmacokinetic parameters and other molecular properties. The total polar surface area, the amount of hydrogen donors, hydrogen acceptors, and rotatable bonds, as well as the compounds' synthetic accessibility, were all reported by the SWISS ADME PREDICTOR. Additionally, Lipinski et al. screens utilizing the SWISS ADME predictor were conducted on the ligands. A pharmacological agent's drug-likeness is an assumption used to determine whether it has characteristics that make it an orally active medication. This prediction is based on the Lipinski rule of five, a theory that Lipinski et. al., have already established. The rule states that when a chemical has more than five H-bond donors, ten H-bond acceptors, a molecular weight larger than 500, and a computed Log P (CLogP) greater than five, the compound considerably has poor absorption or permeability. To select component as drug candidates drug score is the parameter utilized. The probability of a chemical being regarded as a drug candidate increases with the drug score value. (Tian S. et. al., 2015).

3. Results and Discussion

The current investigation was done to comprehend the drug likeness character and their binding orientation towards the target as per shown in table no3. All the selected marketed drug such as Chloroquine, Hydroxychloroquine, Lopinavir/ Ritonavir, Anakinra, Favipiravir, Ribavirin, Baricitinib, Tofacitinib, Remdesivir, Ribavirin, Acalabrutinib, Ibrutinib screened for their ADMET parameter and docked with selected target presented in table no 1.(Zhou YW. et. al., 2021).

Table 1: Selected Marketed drugs used in therapy of COVID -19.

Compound	Structure	Compound	Structure
A1	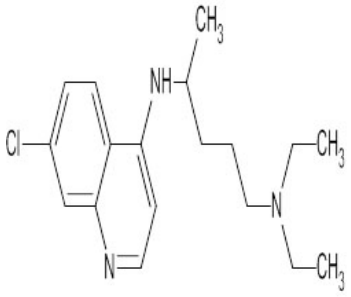	A7	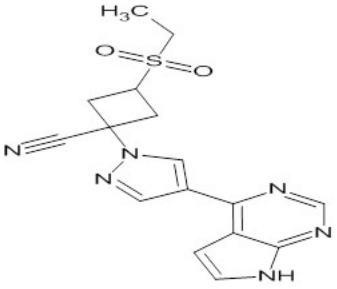
A2	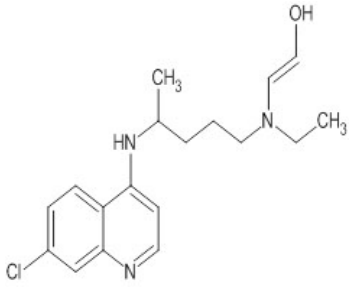	A8	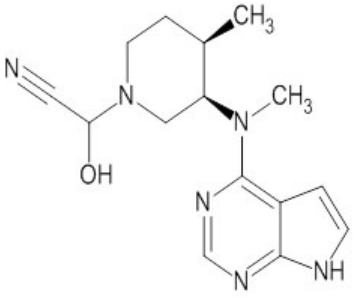
A3	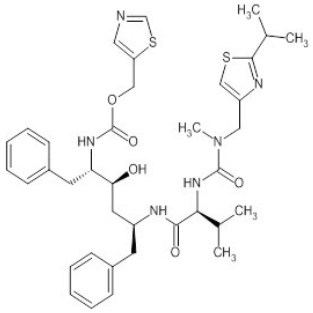	A9	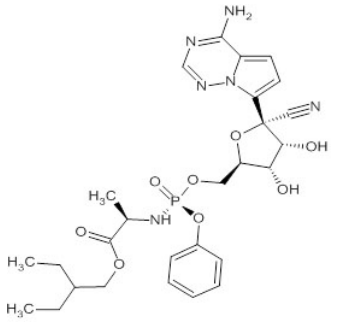

A4	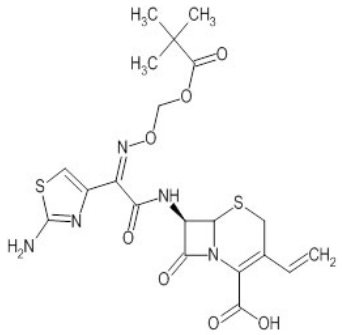	A10	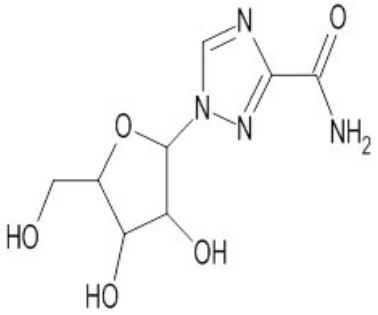
A5	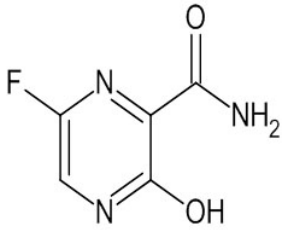	A11	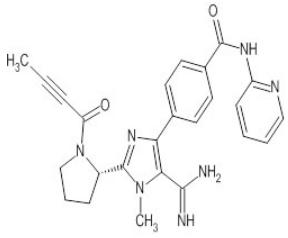
A6	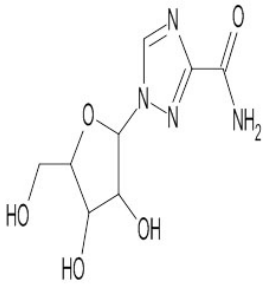	A12	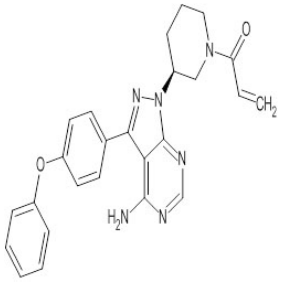

Table 2: In Silico ADMET screening for drugs used in therapy of COVID-19.

Compound	**M.F.**	**M.W.**	**nHBA**	**nHBD**	**Log P**	**TPSA** (A°)	**Rule of Five**
Accepted values	----------	**<500 g/mol**	**<5**	**<10**	**<5**	**<110**	**Max 4**
A1	$C_{18}H_{26}ClN_3$	319.87	2	1	4.32	28.16	4
A2	$C_{18}H_{26}ClN_3O$	335.87	3	2	3.73	48.39	4
A3	$C_{37}H_{48}N_4O_5$	628.80	5	3	2	120.00	4
A4	$C_{20}H_{23}N_5O_7S_2$	509.56	9	3	1.52	227.05	3
A5	$C_5H_4FN_3O_2$	157.10	4	2	0.69	88.84	4
A6	$C_8H_{12}N_4O_5$	244.20	7	4	-2.90	143.72	4
A7	$C_{16}H_{17}N_7O_2S$	371.42	7	1	0.61	128.94	4
A8	$C_{16}H_{20}N_6O$	312.37	4	1	1.04	88.91	4

A9	$C_{27}H_{35}N_6O_8P$	602.58	12	4	-0.05	213.36	3
A10	$C_8H_{12}N_4O_5$	244.20	7	4	-2.90	143.72	4
A11	$C_{26}H_{23}N_7O_2$	465.51	5	2	2.02	118.51	4
A12	$C_{25}H_{24}N_6O_2$	440.50	5	1	2.59	99.16	4

Chloroquine :

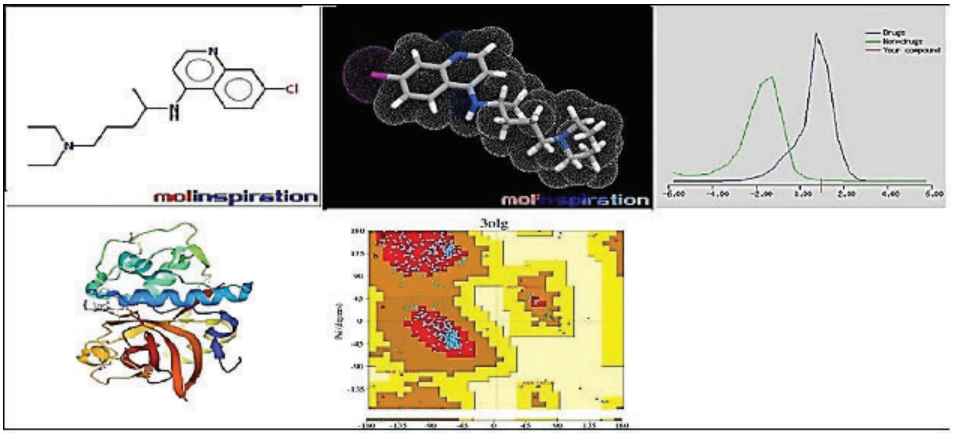

Figure 1: 2D, 3D, drug likeness profile, protein chain and Ramachandran Plot of Chloroquine

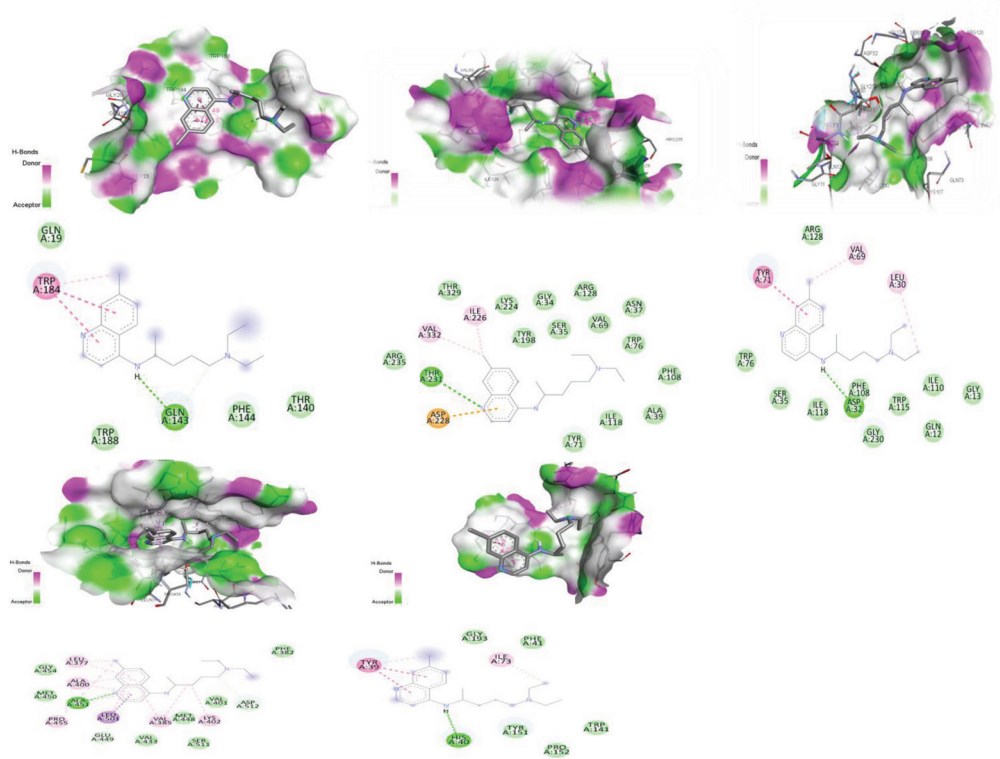

Figure 2: Interaction of Chloroquine with 3O1G,4B72,4B78,4YJU,5LH4.

Hydroxychloroquine

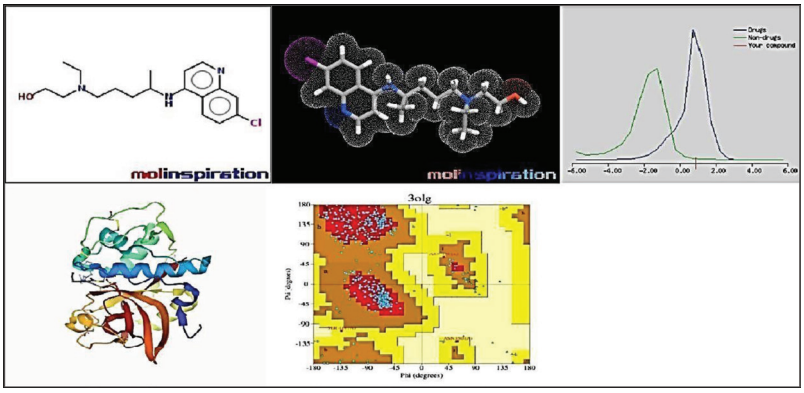

Figure 3: 2D, 3D, drug likeness profile, protein chain and Ramachandran Plot ofHydroxychloroquine.

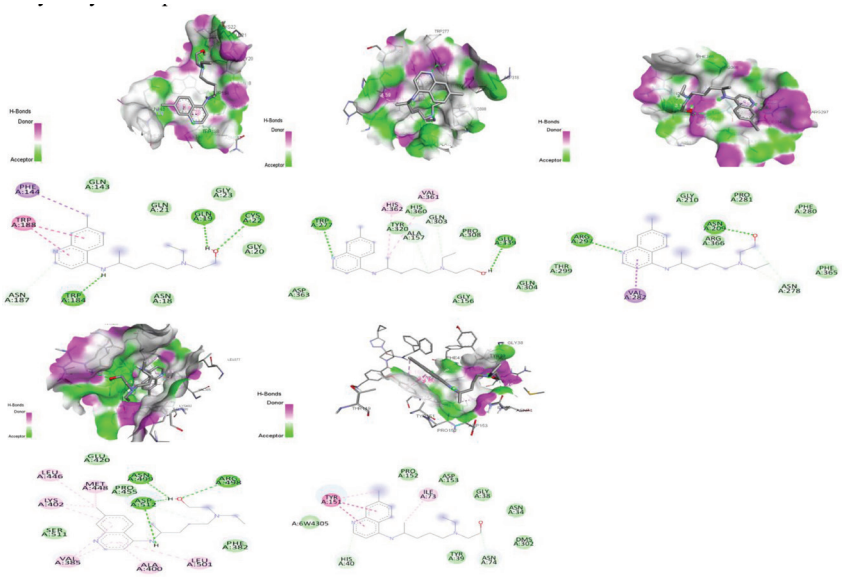

Figure 4: Interaction of Hydroxychloroquine with 3O1G, 4B72,4B78,4YJU, 5LH4.

Lopinavir/Ritonavir

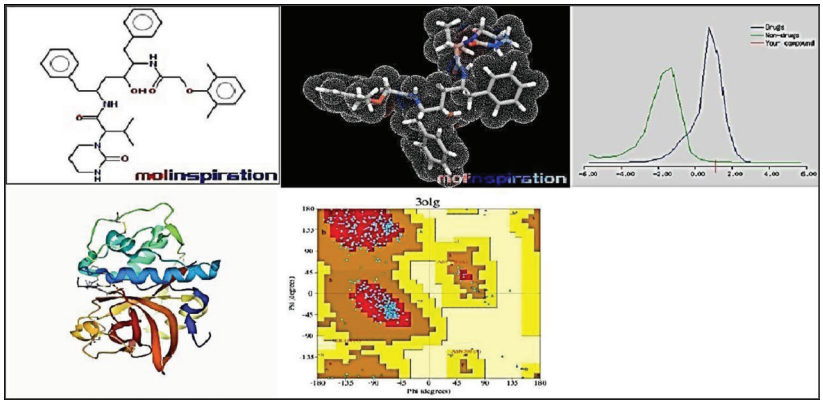

Figure 5: 2D, 3D, drug likeness profile, protein chain and Ramachandran Plot of Lopinavir/Ritonavir.

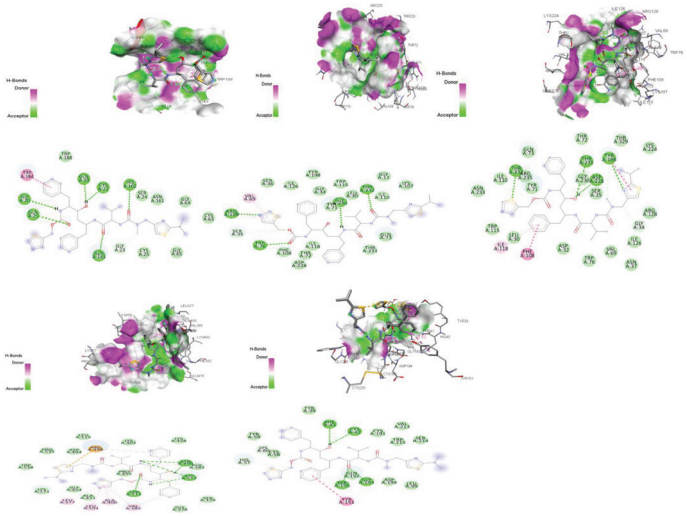

Figure 6: Interaction of Lopinavir/ Ritonavir with 3O1G, 4B72,4B78,4YJU, 5LH4.

Anakinra

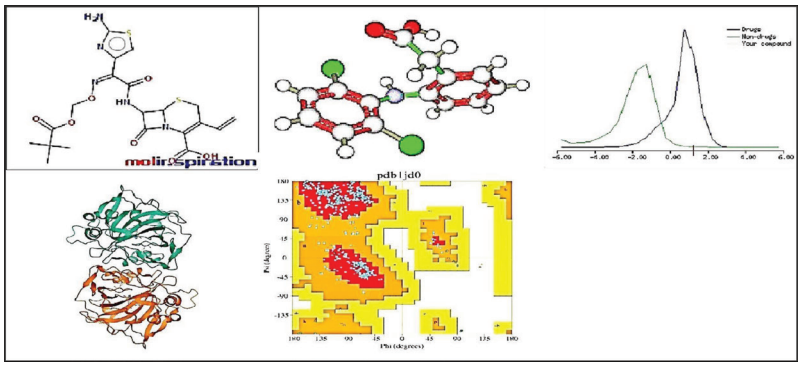

Figure 7: 2D, 3D, drug likeness profile, protein chain and Ramachandran Plot of Anakinra.

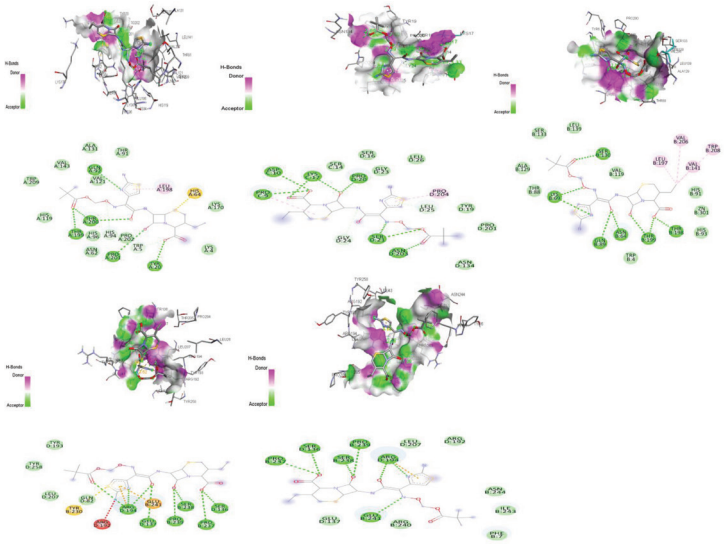

Figure 8: Interaction of Anakinra with 1JD0,4QJ0,4QJW,6G5L,6G7A.

Favipiravir

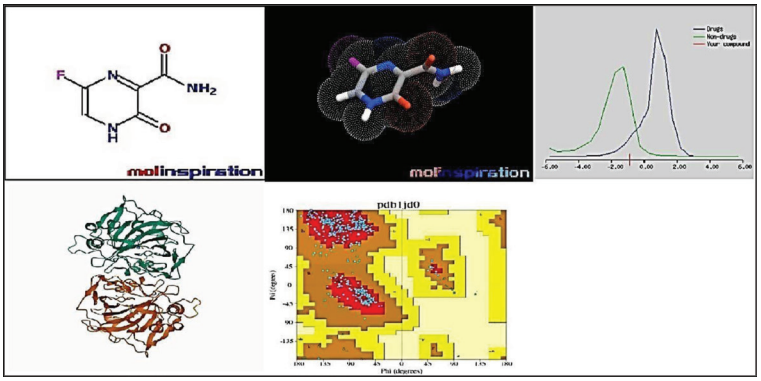

Figure 9: 2D, 3D, drug likeness profile, protein chain and Ramachandran Plot of Favipiravir.

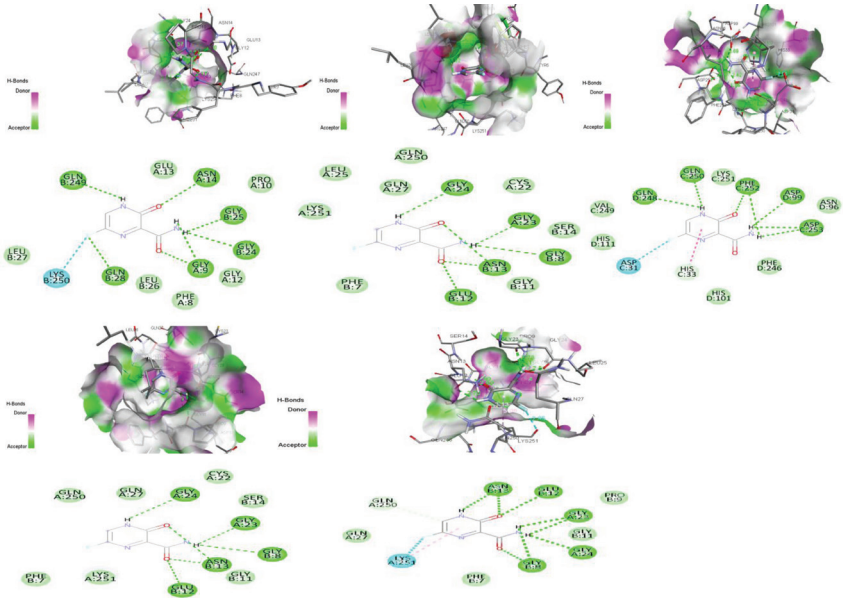

Figure 10: Interaction of Favipiravir with 1JD0,4QJ0,4QJW,6G5L,6G7A.

Ribavirin

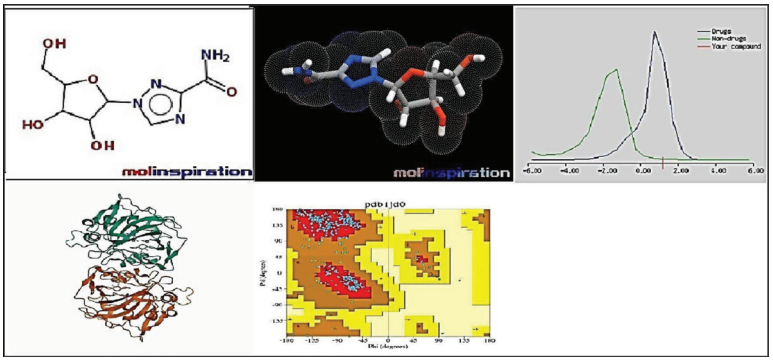

Figure 11: 2D, 3D, drug likeness profile, protein chain and Ramachandran Plot of Ribavirin.

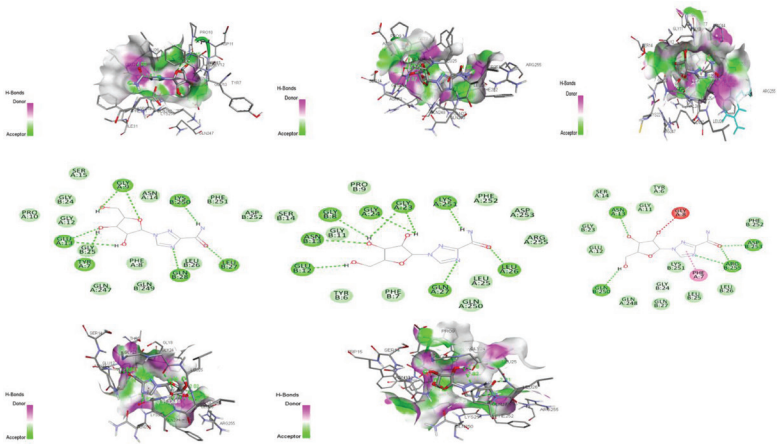

Figure12: Interaction of Ribavirin with 1JD0,4QJ0,4QJW,6G5L,6G7A.

Baricitinib

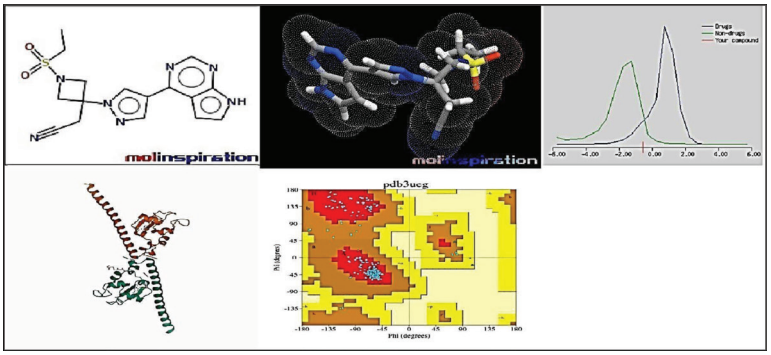

Figure 13: 2D, 3D, drug likeness profile, protein chain and Ramachandran Plot of Baricitinib.

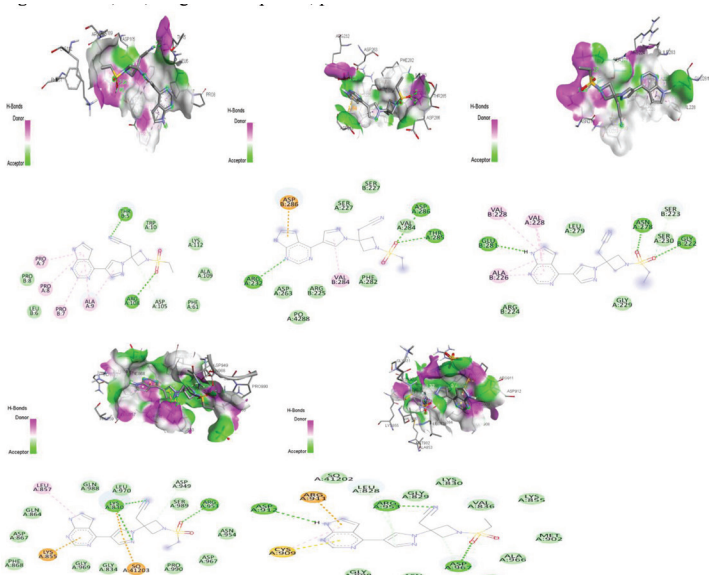

Figure 14: Interaction of Baricitinib with 3UEG,3UGD,3UGI,5TTU,6DUD.

Tofacitinib

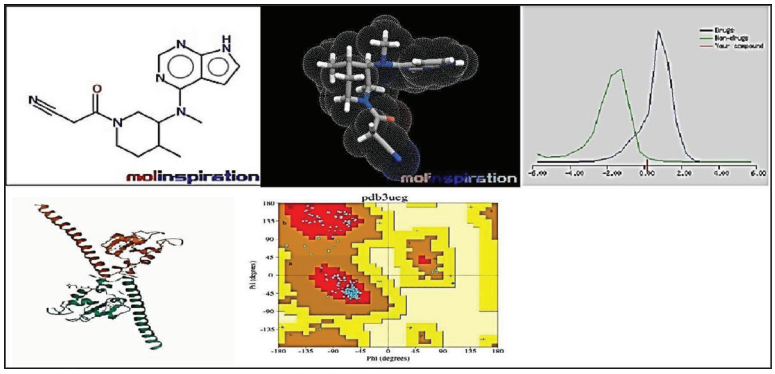

Figure 15: 2D, 3D, drug likeness profile, protein chain and Ramachandran Plot of Tofacitinib.

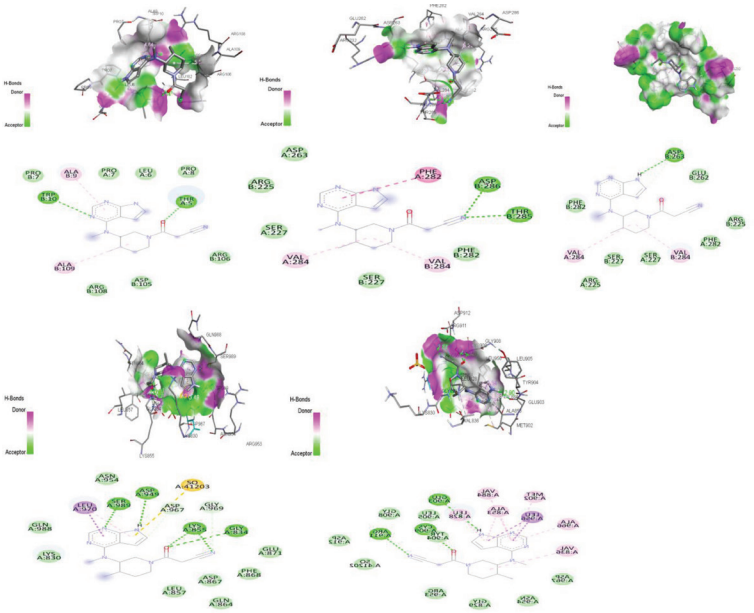

Figure 16: Interaction of Tofacitinib with 3UEG,3UGD,3UGI,5TTU,6DUD.

Remdesivir

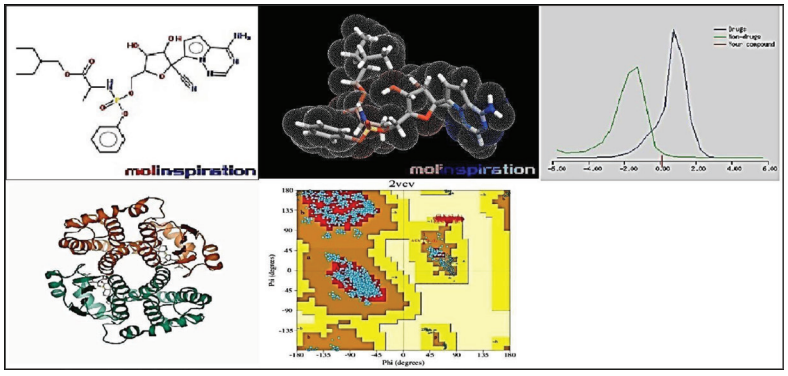

Figure 17: 2D, 3D, drug likeness profile, protein chain and Ramachandran Plot of Remdesivir.

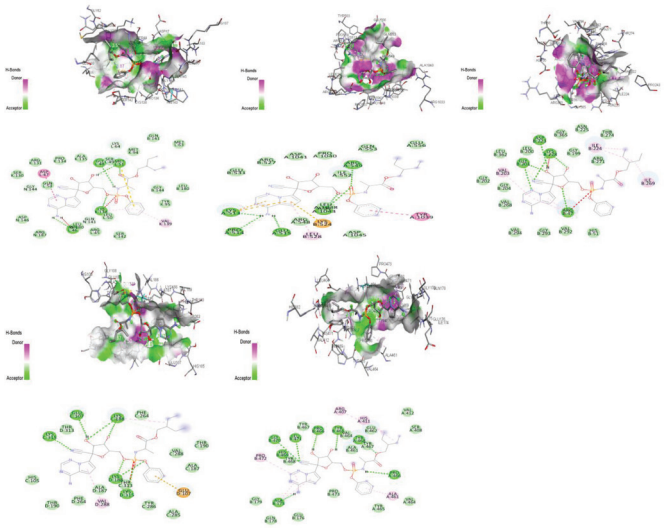

Figure 18: Interaction of Remdesivir with 2VCV,3L9W,5VLO,.5VN1,6NSD.

Ribavirin

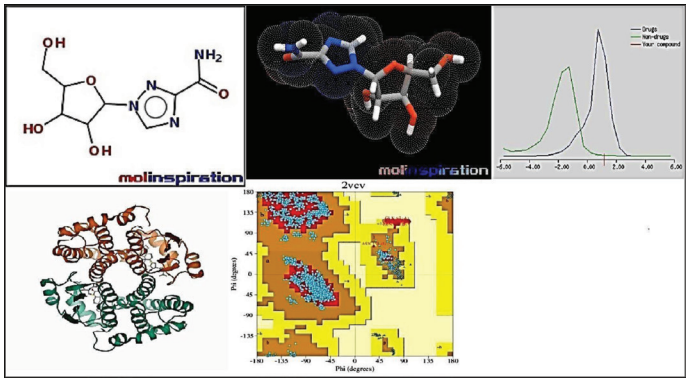

Figure19: 2D, 3D, drug likeness profile, protein chain and Ramachandran Plot of Ribavirin.

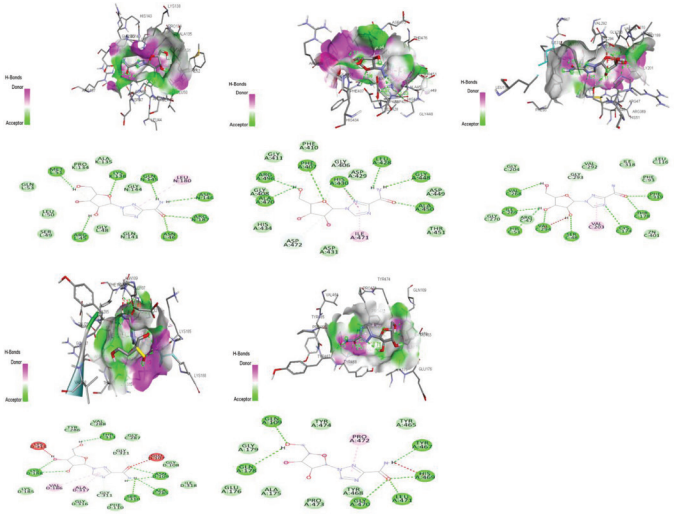

Figure 20: Interaction of Ribavirin with 2VCV,3L9W,5VLO,.5VN1,6NSD.

Acalabrutinib

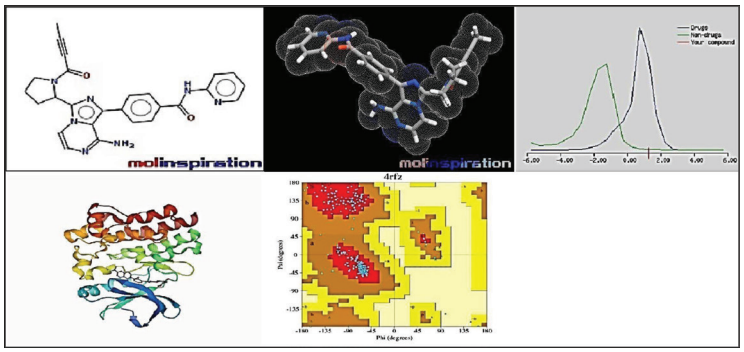

Figure 21: 2D, 3D, drug likeness profile, protein chain and Ramachandran Plot of Acalabrutinib.

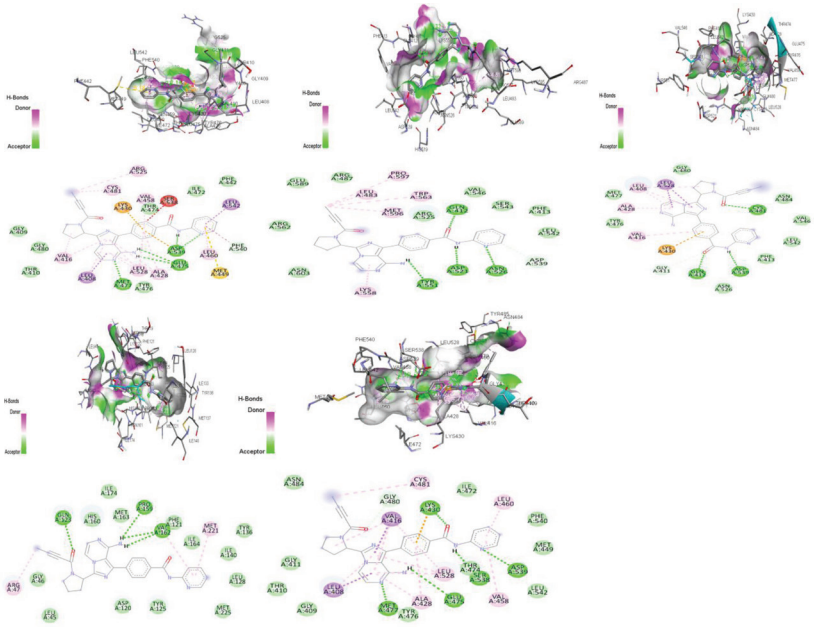

Figure 22: Interaction of Acalabrutinib with 4RFZ, 5JRS, 5KUP, 5OTQ, 5P9I.

Ibrutinib

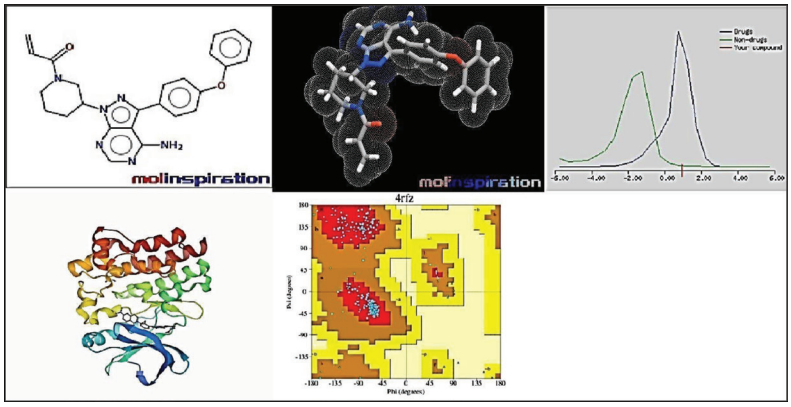

Figure23: 2D, 3D, drug likeness profile, protein chain and Ramachandran Plot of Ibrutinib.

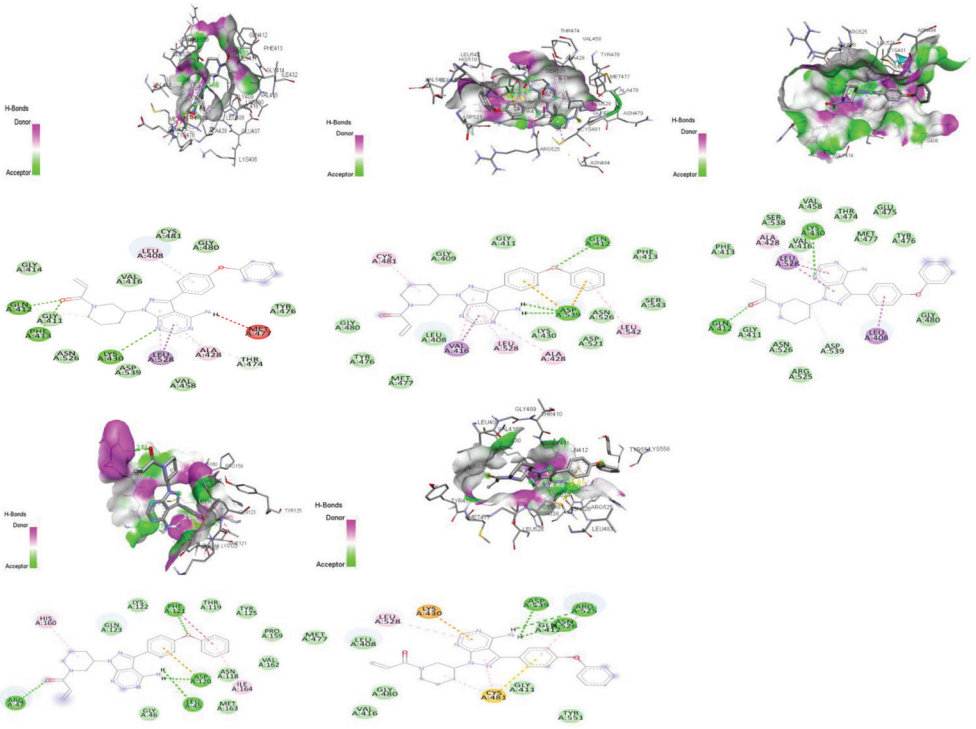

Figure 24: Interaction of Ibrutinib with 4RFZ, 5JRS, 5KUP, 5OTQ, 5P9I.

Table 3: Docking score of marketed API's.

Compound	Protein (PDB)	Free Binding Energy (Kcal/Mol)	Type of Bond Interacted	Interaction group	Length
Chloroquine	3o1g	-5.4	H -Bond	A: GLY143	2.46168
	4b72	-6.2		A: THR231	2.77907
	4b78	-6.1		A:ASP32	2.39614
	4yju	-6.5		A: ALA451	2.05554
	5lh4	-5.5		A: HI540	2.7183
Hydroxychloroquine	3o1g	-5.5		A:CY522	3.00536
				A: TRP184	2.27553
				A: GLN19	2.264667
	4b72	-5.3		A: TRP277	2.48143
				A: GLU339	2.6003
	4b78	-5.3		A: ASN209	1.84875
				A: ARG297	2.40031
				A: ARG297	2.32555

	4yju	-6.4		A: ARG498	2.9807
				A:ASP512	2.41471
				A: ASN499	2.38916
				A:ASP512	2.19627
				A:ASP512	2.85467
	5lh4	-5.3		A: SFR150	2.4223
				A: TYR151	2.55253
				A: TYR151	2.20136
				A: TYR151	4.76442
Lopinavir/ Ritonavir	3o1g	-5.3		A: GLN21	2.56724
				A: GLN143	1.83185
				A: HIS162	2.28239
				A: GLY20	2.54214
				A: GLN19	1.88446
				A: CYS22	2.69104
	4b72	-7.4		A: TRP76	2.40572
				A: ARG128	2.52993
				A: THR232	2.29953
				A: GLY230	1.90131
				: UNK0:H	2.05647
	4b78	-8.6		A: TYR198	2.43023
				A: THR231	2.85818

				A: THR232	2.71301
				A:ASP228	2.52115
	4yju	-6.9		A: SER511	2.55929
				A: ASN499	2.82011
				A:ASP512	2.94867
				A:ASP512	2.26642
				A: ASN499	2.06884
	5lh4	-6.4		A: GLY193	2.01169
				A: SER195	2.33079
				A: PHE41	2.57026
				A: CYS42	2.65049
Anakinra	1jd0	-7.2		A: GLN92	3.0083
				A: THR199	2.47796
				A: THR200	2.45805
				A: THR200	1.63865
				A:PRO201	3.33946
				A: THR200	3.14493
				A: TYR200	2.81364
	4qj0	-7.1		C: LYS17	2.25553
				C: LYS17	2.52588
				C: LYS17	2.52537
				C: LYS17	2.17184

				D: SER21	2.50066
				D: SER21	2.09412
				D: ASN203	2.72549
				D: ASN203	2.690065
				D:PRO20	3.30279
				C:PRO9	3.23637
				C:ASP10	3.33155
	4qjw	-7.9		B: ASN64	2.35848
				B: LYS69	3.06437
				B: LYS69	1.98853
				B: GLN89	2.53918
				B: SER130	2.03951
				B: THR198	2.06306
				B: THR198	2.08358
				B: THR199	2.55739
				B: THR199	2.06078
				B: THR199	2.99297
	6g5l	-7.3		B: SER238	2.19008
				D: ARG194	2.28137
				D: ARG194	2.8782
				D: ARG194	2.59686
				B:PRO239	2.9808

				D: GLU137	3.31434
				B:PRO237	3.19083
				D: SER136	2.91889
	6g7a	-6.9		B: SER238	1.98003
				D: ARG194	2.11788
				D: ARG194	2.77531
				B:PRO239	3.17871
				B: GLU241	3.31003
				B:PRO237	3.05346
				D: SER136	2.94599
Favipiravir	1jd0	-5.9		A: GLY9	2.1662
				A: ASN14	2.89543
				B: GLN28	2.53941
				B: GLN249	2.27826
				A: GLY9	2.34024
				B: GLY24	2.57187
				B: GLY25	2.14674
	4qj0	-6.1		B: GLU12	2.56473
				B: ASN13	1.75972
				B: ASN13	2.39973
				A: GLY24	2.81996
				A: GLY23	2.18943

				B: GLY8	2.81141
	4qjw	-5.8		C: PHE252	1.95586
				C: GLN250	2.23982
				D: GLN248	2.80564
				C:ASP253	2.77665
				D:ASP99	2.69461
				C: PHE252	2.86646
				C:ASP253	2.9378
				: UNK0	2.41687
	6g5l	-6.2		B: GLU12	2.54058
				B: ASN13	1.8298
				B: ASN13	2.48327
				A: GLY24	2.94426
				A: GLY23	2.35992
				B: GLY8	2.86895
	6g7a	-6.1		B: GLY8	1.88558
				B: GLU12	2.59958
				B: ASN13	1.89643
				B: ASN13	2.70138
				A: GLY23	2.7315
				B: GLY8	2.60556
				A: GLY23	2.68238

				A: GLY24	2.5138
Ribavirin	1jd0	-7.2		A: GLY9	2.88358
				A: GLU13	2.31153
				B: LEU27	2.00367
				B: GLN28	2.42314
				A: GLY9	2.14996
				B: LYS250	1.99688
				A: TYR7	2.59906
				A: GLU13	2.48956
	4qj0	-7.5		A: LEU26	1.90179
				A: GLN27	2.50865
				A: ASN13	2.87341
				B: GLU12	2.30233
				A: LYS251	2.18037
				A: GLY23	2.75191
				B: GLY8	2.36204
				A: GLY23	2.2517
				A: GLY24	2.61738
	4qjw	-7.9		A: ASN13	2.25988
				B:ASP253	1.97699
				B: ARG255	3.04921

				B: ARG255	2.52334
				B: ARG255	1.95813
				B: GLN250	2.39504
	6g5l	-7.2		A: LEU26	2.02304
				A: GLN27	1.74015
				A: LYS251	2.81994
				A:ASP253	1.87648
				B: GLU12	2.49726
				B: ASN13	2.04573
				B: TYR6	2.63005
				B: GLU12	2.94132
				A: GLY24	2.69183
	6g7a	-6.4		C: LYS17	2.30323
				C: LYS17	2.25957
				C: SER14	2.33075
				C:ASP10	2.74771
				C:PRO9	2.36663
				C:ASP10	3.0268
	3ueg	-6.0		A: ARG108	2.95789
				A: ARG108	2.95855
				B: THR5	2.16809
				B: THR5	2.58512

Baricitinib	3ugd	-5.5		A: ARG232	3.05442
				A: THR285	2.56436
				A:ASP286	2.76568
	3ugi	-5.8		A: ASN278	1.85658
				B: GLY222	2.36746
				B: GLU281	2.30342
	5ttu	-6.8		A: LYS830	2.89973
				A: LYS830	2.25914
				A: LYS830	3.00644
				A: ARG953	2.40122
	6dud	-7.4		A: ARG953	2.1402
				A: ARG953	2.20164
				A:ASP967	2.44469
				A:ASP912	2.86059
Tofacitinib	3ueg	-5.4		A: THR5	1.81356
				A: THR5	2.14319
				B: TRP10	3.05986
	3ugd	-5.7		B: THR285	2.4026
				B:ASP286	2.84877
	3ugi	-6.0		B:ASP263	2.54883
	5ttu	-7.0		A: GLY834	3.07267
				A: LYS855	2.35992

				A: LYS855	2.9973
				A: SER989	1.98125
				A:ASP949	2.32687
	6dud	-7.0		A: CYS909	2.47658
				A: CYS909	2.95294
				A: ARG911	2.67168
				A: GLU903	2.89649
Remdesivir	2vcv	-8.4		K: LYS138	1.95143
				L: MET51	2.8226
				L: ASN46	2.89301
				L: MET51	2.59307
				L: GLY48	2.17681
	3l9w	-7.9		A: ARG549	2.54481
				A: ARG549	2.75993
				A: ASN1043	3.01959
				A: ASN1043	2.29125
				A: GLU515	2.1476
				A: LYS513	2.21556
				A:PRO514	2.73707
	5vl0	-8.0		B: ARG47	2.36627
				B: GLY201	2.80776
				B: GLY201	2.45727

				B: LYS228	2.59623
				B: LYS228	2.11711
				B:ASP223	2.86963
	5vn1	-7.4		C: LYS188	3.04554
				C: LYS188	2.08119
				C: LYS315	2.49133
				D: LYS188	2.65953
				D: LYS188	2.19026
				D: LYS315	2.59218
				C: GLU107	2.73123
				: UNK0	2.16623
	6nsd	-8.9		A: TYR468	1.96936
				B: HIS469	2.13624
				B: HIS469	3.03306
				B: GLY470	3.06853
				B: LEU471	2.6574
				B: ALA175	1.90186
				B:PRO466	2.71816
				B: TYR465	2.48049
				A:PRO466	2.39593
	2vcv	-7.1		K: LYS138	2.7303
				L: ASN46	2.47955

				D: LYS188	2.29363
				D: LYS188	2.18287
				C: THR313	1.99419
				C: ALA285	2.68892
				C: SER310	2.67309
				D: ASN109	2.27361
	6nsd	-6.4		A: GLN109	2.28214
				A: HIS469	1.8636
				A: GLY470	2.50874
				A: LEU471	2.07516
				A: GLN178	2.70592
				A: TYR467	2.14583
				: UNK0:H	2.75333
	4rf2	-8.8		A: MET47	2.4109
				A:ASP53	2.7709
				A:ASP39	2.13559
				A: GLU75	2.9222
				A: GLU475	2.71273
	5jrs	-8.5		A: GLN412	2.90532
				A: ASN526	2.66237
				A:ASP21	2.54633
				A: TYR551	2.32238

Acalabrutinib	5kup	-9.1		A: GLN412	2.48308
				A: CYS481	2.39473
				A: CYS481	2.34248
				A:ASP539	2.36967
	5otq	-10.0		A: GLN123	2.47856
				A:PRO159	2.76708
				A: VAL162	2.70571
				A: VAL162	2.66234
	5pqi	-8.5		A: LYS430	2.59044
				A: MET477	2.40773
				A:ASP539	2.37513
				A: SER538	2.6957
				A: GLU475	2.81159
Ibrutinib	4rfz	-8.0		A: GLN412	2.07576
				A: PHE413	2.63186
				A: LYS430	2.88324
	5jrs	-9.5		A: GLN412	2.26099
				A:ASP539	2.46341
				A:ASP539	2.62578
	5kup	-9.2		A: GLN412	2.13073
				A: LYS430	2.8115
	5otg	-7.8		A: ARG47	2.61265
				A: PHE121	2.02163
				A: LEU45	2.74451
				A:ASP120	2.88295
	5pqt	-8.8		A: ARG525	2.91633
				A: ASN526	2.49581
				A:ASP539	2.55558

Conclusion

The rule of five (RO5), also referred to as Lipinski's rule of five, Pfizer's rule of five, or simply the rule of five, is a general guideline used to assess how similar a chemical compound is to an existing drug or to ascertain whether it possesses chemical and physical characteristics that would make it likely to be an orally active drug in humans. The rule specifies molecular characteristics crucial for a drug's pharmacokinetics i.e., its absorption, distribution, metabolism, and excretion ("ADME") in the human body. The rule is essential to remember when a pharmacologically active lead structure is progressively optimized during drug discovery in order to increase the activity and selectivity of the compound and to guarantee that Lipinski's rule-described drug-like physicochemical features are maintained. On the basis of result obtained from ADMET as well as docking study of all marketed selected drugs used in therapy of COVID-19, it predicted or concluded that drugs such as Chloroquine, Hydroxychloroquine, Lopinavir/ ritonavir, Favipiravir, Ribavirin, Baricitinib, Tofacitinib, Acalabrutinib, Ibrutinib follows Lipinski rule of five except Anakinra and Remdesivir. Also showing good affinity towards the Targets (3O1G, 4B72, 4B78, 4YJU, 5LH4, 1JDO, 4QJO, 4QJW, 6G5L, 6G7A, 3UEG,3UGD, 5TTU, 6DUD, 2VCV, 3L9W, 5VLO, 5VN1, 6NSD, 4RFZ, 5JRS, 5KUP, 5OTQ, 5P9I). The binding energy of the protein ligand interaction additionally conforms that the ligand fit into the dynamet pockets.

Acknowledgements:

The authors are thankful to Dr. Shivajirao Kadam College of Pharmacy Kasabe Digraj, Sangli, Maharashtra, India, for providing research facilities to do work and their constant support during work.

Funding

No funding was received in association with this manuscript.

Conflict of Interest

The authors declare that they have no known competing financial interests or personal relationships that could have appeared to influence the work reported in this paper.

Declaration

It is an original data and has neither been sent elsewhere nor published anywhere.

Authorship Contribution

Manuscript preparation and practical work: Ms. Payal P Chavan, Ms. Supriya S Shete, Ms. Dipti S Patil, Mr. Saroj D Kolekar.
Practical guidance and helping in manuscript writing: Mr. Godfrey R Mathews, Mr. Dipak B Bhingardeve, Mr. Pravin K Pawar.
Whole guidance for project: Mr. Sagar A Jadhav.

References

Antonopoulou, lo, Sapountzaki E., Rova U (2022). Inhibition of the main protease of SARS-Cov-2[m^{pro}] by repurposing/designing drug like substances and utilizing nature´s toolbox of bioactive compounds. *Comput Struct Biotechnol J*., 20, 1306-1344. https://doi.org/10.1016/j.csbj.2022.03.009

Bojarska J., Remko M., Breza M. (2020). A Supramolecular Approach to Structure -Based Design with A Focus on Synthons Hierchy in Ornithine-Derived Ligands: Review, Synthesis, Experimental and in Silico Studies *Molecules*, 25(5), 1135. https://doi.org/10.3390/molecules 25051135.

Eknis S., Mestres J., Testa B.(2007). In silico pharmacology for drug discovery: methods for virtual ligand screening and profiling. *Br J Pharmacol*, 1152(1), 9-22. https://doi.org/10.1038/sj.bjp.0707305.

Herowati R., Widodo G. P. (2014). Molecular Docking Studies of Chemical Constituents of Tinospora cordifolia on Glycogen phosphorylase. *Procedia Chemistry*, 13, 63-68. https://doi.org/10.1016/j.proche.2014.12.007.

Homayun B., Lin X., Choi H. J. (2019). Challenges and Recent Progress in Oral Drug Delivery Systems for Biopharmaceuticals, *Pharmaceutics*, 11(3)129. https://doi.org/10.3390/pharmaceutics11030129.

Lin J, Sahakian D. C., de Morais S.M., Xu J. J., Polzar R.J, Winter S.M. (2003). The role of absorption, distribution, Metabolism, excretion and toxicity in drug discovery. *Curr Top Med Chem*., *3*(10), 1125-54 https://doi.org/10.2174/15680260334512096.

Malik Y. A. (2020). properties of Coronavirus and SARS-CoV-2. *Malays J Pathol*, *42*(1), 3-11.

Morris G.M, Lim-Wilby M, (2008). Molecular docking Methods. *Mol Biol*, *443*, 365-82. https://doi.org/10.1007/978-1-59745-177-2_19.

Pal M., Berhanu G., Desalegn C., (2020). Severe Acute Respiratory Syndrome Coronavirus-2 (SARS-CoV-2) An Update. *cureus*,*12*(3), e7423. https://doi.org/10.7759/cureus.7423

Rauf M. A., Zubair S., Azhar A., (2015). Ligand docking and binding site analysis with Pymol and autodock / vina. I*nternational Journal of Basic and Applied Sciences*, *4*(2),168-177. https://doi.org/10.14419/ijbs.v4i2.4123

Sharma A., Tiwari S., Deb M. K., Marty J. L. (2020). Severe acute respiratory syndrome coronavirus -2(SARS-CoV-2): a global pandemic and treatment strategies. *Int J Antimicrob Agents*, *56*(2),106054. https://doi.org/10.1016/j.ijantimicag.22.106054

Srivastav V., Yadav A., Sarkar p. (2022). Molecular docking and ADMET study of bioactive Compound of Glycyrrhiza glabra against main protease of SARS-COV2, *Mater Today Proc*, *49*(8), 2999-3007. https://doi.org/10.1016/j.matpr.2020.10.055

Tian S., Wang J., Li Y., Li D., Xu L., Hou T. (2015). The application of in silico drug-likeness predictions in pharmaceutical research, *Adv Drug Deliv Rev*, *23*, 86, 2-10. https://doi.org/10.1016/j.addr.2015.01.009.

Trott O., Olson A. J. (2010). Autodock Vina: improving the speed and accuracy of docking with a new scoring functions,efficient optimization ,and multithreading. *J Comput Chem*, *31*(2), 455-61. https://doi.org/10.1002/jcc.21334

Vardhan S., Sahoo S. K. (2020). In silico ADMET and molecular docking study on searching potential inhibitors from limonoids and triterpenoids for COVID-19. *Comput Bio Med*;103936 https://doi.org/10.1016/j.compbiomed.22103936.

V´Kovski P., Kratzel A., Steiner S. (2021). Coronavirus biology and replication:implications for SARS-CoV-2. *Nat Rev Microbiol*, *19*, 155-170. https://doi.org/10.1038/s41579-020-00468-6

Zheng J. (2020). SARS-CoV-2:an Emerging Coronavirus that Causes a Global Threat. *Int J Biol Sci*, *16*(10),11678-1685. https://doi.org/10.7150/ijbs.45053

Zhou Y. W., Xie Y., Tang L. S., Pu D., Zhu Y. J., Liu J. Y. (2021). Therapeutic targets and interventional strategies in COVID-19: mechanism and clinical studies. *Signal Transduct Target Ther*, *6*(1), 317 https://doi.org/10.1038/s41392-02100733-x

CHITKARA

Journal of Pharmaceutical Technology, Research and Management

Chitkara University, Saraswati Kendra, SCO 160-161, Sector 9-C, Chandigarh, 160009, India

Volume 10, Issue 1 **May 2022** **ISSN 2321-2217**